Applying a Flexible Microactuator to Robotic Mechanisms

Koichi Suzumori, Shoichi Iikura, and Hiroshisa Tanaka

A flexible microactuator (FMA) driven by an electro-pneumatic (or electro-hydraulic) system has been developed. It has three degrees of freedom — pitch, yaw, and stretch — making it suitable for robotic mechanisms such as fingers, arms, or legs. It is made of fiber-reinforced rubber and the mechanism is very simple, enabling gentle miniature robots without conventional link mechanisms to be designed.

Serially connected FMAs act as a miniature robot manipulator. The kinematics and control algorithm for this type of robot are presented. On the other hand, FMAs combined in parallel act as a multi-fingered robot hand. Each FMA represents a finger. An algorithm for the cooperative control of such FMAs, the stable region for holding, and its performance have been developed.

Nonindustrial Robot Applications

Recently, attempts have been made to apply robots in a variety of fields, not only industrial areas but also non-industrial areas such as medicine, biology, and agriculture [1]. Examples of these are medical micro-robots for inspecting the body or supporting microsurgery, and robots with soft grips for handling fragile items such as eggs, fruit, or glasses. However, it is not easy to create such robots using conventional machine elements (especially actuators) and conventional robot design techniques based on rigid link mechanisms.

The FMA basic characteristics have already been reported [2]-[4]. This paper describes the design and control methods used in applying FMAs to robotic mechanisms. First, the FMA mechanism and basic characteristics are presented. After that, two applications to miniature robotic mechanisms are discussed; one is a manipulator and the other is a multi-fingered robot hand.

Presented at the 1991 IEEE International Conference on Robotics and Automation, Sacramento, CA, April 9-11, 1991. *K. Suzumori and S. Iikura are with the Research and Development Center, Toshiba Corporation, 4-1, Ukishima-cho, Kawasaki-ku, Kawasaki 210, Japan. H. Tanaka is with the Dept. of Mechanical Engineering, Yokohama National University, Yokohama, Japan.*

FMA Mechanism

In general, rubber actuators can be divided into two classes, shrink and stretch categories [5],[6]. An FMA can be regarded as a special version of the stretch category.

The FMA structure is shown in Fig. 1. It is made of fiber-reinforced rubber. Its deformation is controlled by an electro-pneumatic (or electro-hydraulic) pressure control system. There are three internal chambers, whose individual internal pressures are controlled independently through flexible tubes, which are connected to pressure control valves. The FMA is reinforced with fiber in the circular direction, as shown in Fig.1. Thus, it easily deforms in the axial direction, while it resists deformation in the radial direction.

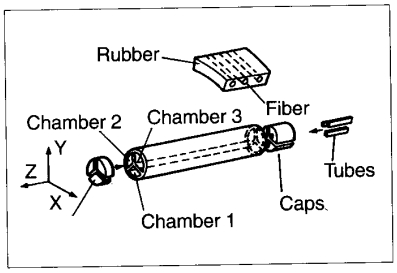

Fig. 1. Structure of FMA.

When the internal pressure in the three chambers is increased equally, the FMA stretches in the axial direction. On the other hand, when the pressure of only one chamber (Chamber 1, for example) is increased, the FMA bends in a direction opposite to the pressurized chamber (in the y direction in this example). The FMA can be bent in any direction by appropriately controllIng the pressure in the three chambers. Thus, the FMA has three degrees of freedom: pitch, yaw, and stretch. Fig. 2 shows the movement of a 1-mm diameter FMA. The developed FMAs range in size from 1 to 20 mm in diameter.

The FMA has several distinctive features, when compared with conventional actuators. 1) It is easy to miniaturize, because of its simple structure. 2) It has a high power density. 3) It has many degrees of freedom, suitable for robot mechanisms. 4) It is cheap. 5) It operates smoothly and gently because of its frictionless mechanism.

Basic Characteristics

Static Characteristics

Approximate characteristic equations for FMAs are presented in this section. They were obtained by linear analysis, based on the theory of infinitesimal elastic deformation.

Fig. 3 shows an analytical model of an FMA. It is assumed that the FMA deformation is small and that it takes the form of an arc. Then, the deformation can be described using the three parameters θ, R, and λ, as shown in Fig. 3. θ represents the bending direction angle, which is defined as the angle between the x-axis and the ξ-axis. Coordinate O-xyz is fixed at the base of the FMA, as shown in Fig. 3, and is ξ the projection of the center axis onto the xy-plane. R is the curvature of the center axis. λ is the angle between the z-axis and the tip direction of the FMA.

By applying the infinitesimal deformation theory, θ, R, and λ can be derived as functions of internal pressure P_i in individual chambers (i = 1,2,3), as follows [2],[3]. First, from the equivalents of the bending moment vectors on the x-y plane, the following equation is obtained:

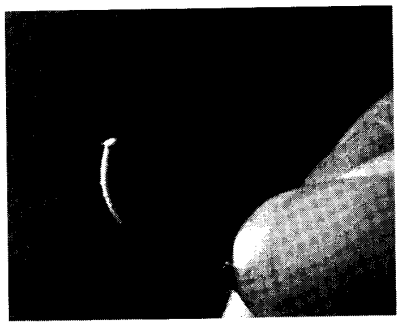

Fig. 2. Movement of 1 mm diameter FMA.

0272-1708/92/$03.00©1992IEEE

$$\tan\theta = \frac{2P_1 - P_2 - P_3}{\sqrt{3}\,(P_2 - P_3)}. \quad (1)$$

Next, the FMA is assumed to be divided into three sectors along the axial direction. Then, from the equivalents of the forces acting on each sector and the boundary conditions between the sectors, the following equations are obtained, where E_t is Young's modulus for the fiber-reinforced rubber in the transverse direction, L_o is the normal FMA length, and L is the current FMA length:

$$R = \frac{3E_t I}{A_p \delta \sum_{i=1}^{3} (p_i \cdot \sin\theta_i)} \quad (2)$$

$$L = \frac{A_p L_o}{3 A_o E_t} \sum_{i+1}^{3} P_i + L_o \quad (3)$$

$$\lambda = L/R. \quad (4)$$

Also, in the FMA cross-section (Fig. 4 shows a cross-section through a 12-mm diameter FMA), I is the moment of inertia for the area, A_p is the pressurized area (total area of the three sectors in Fig. 4), A_o is the area of the fiber-reinforced rubber (white in Fig. 4), and δ is the distance between the FMA center and the center of each fan-shaped area. In this paper, simple characteristic equations are obtained by assuming E_t is a constant with a mean gradient, for from 0 to 50% strain.

In Fig. 5, the calculated characteristics are compared with experimental data for the special case of $P_2 = P_3 = 0$, taken from a 12-mm diameter FMA without a load.

Dynamic Characteristics

The FMA dynamic characteristics are derived theoretically by considering 1) the fluid friction in the flexible tubes between the FMA and its control valves with Hagen-Poiseuille's equation, 2) the fundamental vibration frequency of the rubber, and 3) the compressibility of the working fluid in the FMA chambers [2],[4].

P_{iv} represents the pressure in the output port for the ith valve. L_p is the length of the flexible tubing between the FMA and its pressure control valves, a is the inner diameter of the tubes, and b is the damping coefficient of the FMA. ρ, K, and ν are parameters for working fluid; the density, the bulk modulus, and the kinematic coefficient of viscosity, respectively. Then, the dynamics are expressed by the following transfer function:

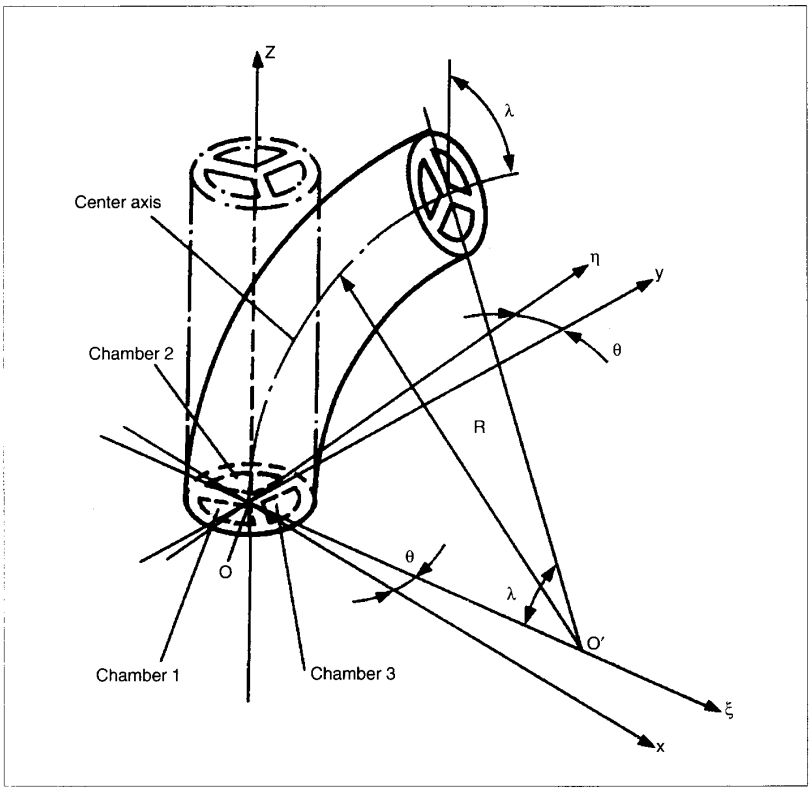

Fig. 3. Analytical model of FMA.

Fig. 4. Cross-section of FMA (12 mm in diameter).

$$\frac{\xi}{P_{ev}} = \frac{B}{A_1 s^3 + A_2 s^2 + A_3 s + 1} \quad (5)$$

where $P_{ev} = \Sigma\,(P_{iv} \sin\theta_i)$, $A_1 = j/\omega^2$, $A_2 = J\,b/\omega + 1/\omega^2$, $A_3 = J + 2\,b/\omega + J\,\alpha$, $J = 8\rho L_p \nu\, A_p\, L_o/(3\,K\,\pi\,a^4)$, $\alpha = A_p\,K/(A_o\,E_t)$, and $B = A_p\,\delta\,L_o^2/(6\,E_t\,I)$.

ω is the fundamental FMA vibration frequency, which is calculated as follows with lateral vibration of a cantilever model, where M_L is the inertia of the load attached to the FMA tip and M_S is the FMA dead weight:

$$\omega = (3\,E_t\,I)^{0.5}\,(M_L + 0.236\,M_S)^{-0.5}\,L^{-1.5}. \quad (6)$$

In Fig. 6, one of the theoretical results is compared with experimental data. The experiment was carried out to measure the response of a 4-mm-diameter 20-mm-long FMA to a step input at the pressure control valves. The response was measured using a light LED attached to the tip of the FMA, and its position was recorded with position sensing devices.

Application to Miniature Robot Arm

An FMA can be used as the arm of a miniature robot. FMA movements pitch, yaw, and stretch are suitable for miniature robot arms. By connecting FMAs serially, an arm is obtained with many degrees of freedom and snake-like movements. Fig. 7 shows a prototype made from two FMAs and a mini-gripper (which is also made of fiber reinforced rubber) [2]. It has seven degrees of freedom including the gripper. Tubes connected to the upper FMA and the gripper pass through the chambers in the lower FMA.

In this section, the kinematics for serially connected FMAs are described, along with a feedback control experiment.

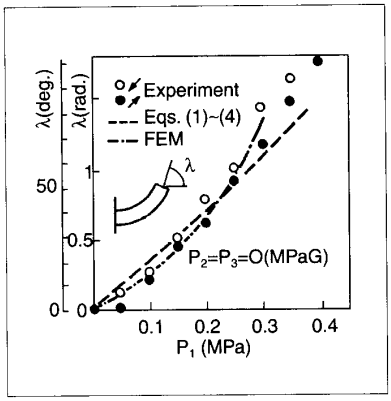

Fig. 5. Static bending characteristics.

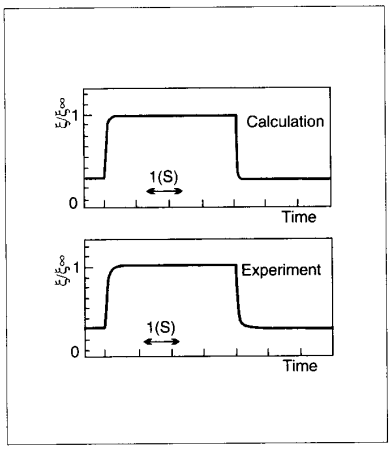

Fig. 6. Step response of 4- mm-diameter 20-mm-long FMA.

Kinematics for Serial Connected FMAs

Fig. 8 shows the configuration of a robot arm made of serially connected FMAs. It has $n \times 3$ degrees of freedom. Each FMA has local coordinates $\Sigma_i\,(O_i - x_i y_i z_i)$ fixed at its base. Its definition is the same as the coordinate shown in Fig.3. d_i is the length of the connection between the ith FMA and the $(i + 1)$th FMA, which is rigid.

By using parameters θ, λ, and R, which are defined in Fig. 3 for the FMA deformation, the Euler angle is expressed as $(\theta, \lambda, -\theta)$. So, a homogeneous transformation matrix A_i from coordinate Σ_i to coordinate Σ_{i-1} is derived as follows:

$$A_i = \begin{bmatrix} C_{\lambda i} C_{\theta i}^2 + S_{\theta i}^2 & S_{\theta i} C_{\theta i} (C_{\lambda i} - 1) & S_{\lambda i} C_{\theta i} & [R_i(1 - C_{\lambda i}) + d_i S_{\lambda i}] C_{\theta i} \\ S_{\theta i} C_{\theta i} (C_{\lambda i} - 1) & C_{\lambda i} S_{\theta i}^2 + C_{\theta i}^2 & S_{\lambda i} S_{\theta i} & [R_i(1 - C_{\lambda i}) + d_i S_{\lambda i}] S_{\theta i} \\ -S_{\lambda i} C_{\theta i} & -S_{\lambda i} S_{\theta i} & C_{\lambda i} & R_i S_{\lambda i} + d_i C_{\lambda i} \\ 0 & 0 & 0 & 1 \end{bmatrix} \quad (7)$$

where $C_{\lambda i} = \cos \lambda_i$, $S_{\lambda i} = \sin \lambda_i$, $C_{\theta i} = \cos \theta_i$, $S_{\theta i} = \cos \theta_i$. Subscript i means the ith FMA.

Compliance Control Experiment

Next, a simple experiment on compliance control, using the transformation matrix shown in (7) is described. Usually, the compliance of a conventional manipulator made of mechanically rigid links is controlled by giving it limpness. On the other hand, the compliance of a manipulator made of FMAs, which is mechanically soft, is controlled by giving it stiffness.

To simplify the experiment, the following conditions were set:

1) Manipulator consists of two FMAs, or $n = 2$.

2) Let $P_{12} = P_{13} = P_{21} = 0$ MPaG and $P_{22} = P_{23}$, so that the manipulator moves only in the y_o–z_o plane. Then, P_{ij} means the internal pressure in the jth chamber for the ith FMA ($i = 1, 2, j = 1, 2, 3$).

3) Controlled values are y_o and z_o representing the manipulator tip position.

A control algorithm is derived by substituting $\theta_1 = \pi/2$ and $\theta_2 = -\pi/2$ into (1)-(4), (7) and the Jacobian matrix derived from (7). The manipulator movement is detected optically, using an LED attached to the tip and a position sensing device. Measured data regarding the LED positions are fed to a computer, and a closed loop with proportional control is constructed.

Fig. 9 shows the experimental compliance control results. It indicates that the FMA manipulator compliance can be controlled by adjusting feedback gain K_f. In this experiment, reference inputs are kept constant. The sampling period for the control system is 50 ms.

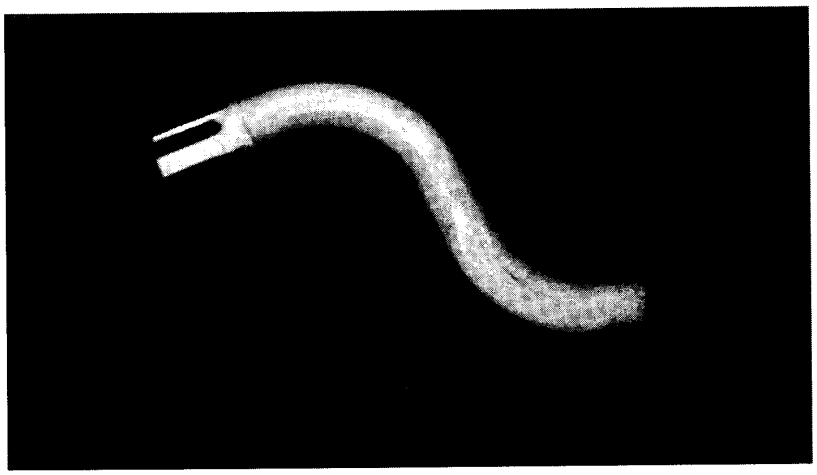

Fig. 7. Manipulator with seven degrees of freedom (120 mm in length).

Application to Multi-Fingered Robot Hand

This section explains a case where FMAs were used to form a multi-fingered robot hand. FMAs enabled a dexterous and soft hand to be created.

In Fig. 10, three holding methods —pinching, pair-pinching, and grasping — are shown for the prototype four-fingered robot hand. The prototype was made of four FMAs, each 12 mm in diameter, and had 12 degrees of freedom.

Control Algorithm

Fig. 11 shows the FMA movements for the three holding modes in Fig.10, a front view of the hand. Global coordinates $\Sigma_o(O_o - x_o y_o z_o)$, based at the center of the hand, and local coordinates $\Sigma_i(O_i - x_i y_i z_i)$ for each FMA (i=1,2,3,4), based at the bottom of the ith FMA, are defined as in Fig. 11.

From the equilibrium condition of bending moments over the cross-section of the FMA, the following approximate equation is obtained:

$$\begin{pmatrix} {}^i x_i \\ {}^i y_i \\ {}^i z_i \end{pmatrix} = \begin{bmatrix} 0 & (\sqrt{3}/2)K_1 & (-\sqrt{3}/2)K_1 \\ K_1 & (-1/2)K_1 & (-1/2)K_1 \\ K_2 & K_2 & K_2 \end{bmatrix} \begin{pmatrix} P_{i1} \\ P_{i2} \\ P_{i3} \end{pmatrix} \quad (8)$$

where ${}^i x_i$, ${}^i y_i$, and ${}^i z_i$ mean the movements of the ith FMA tip, expressed in local coordinates

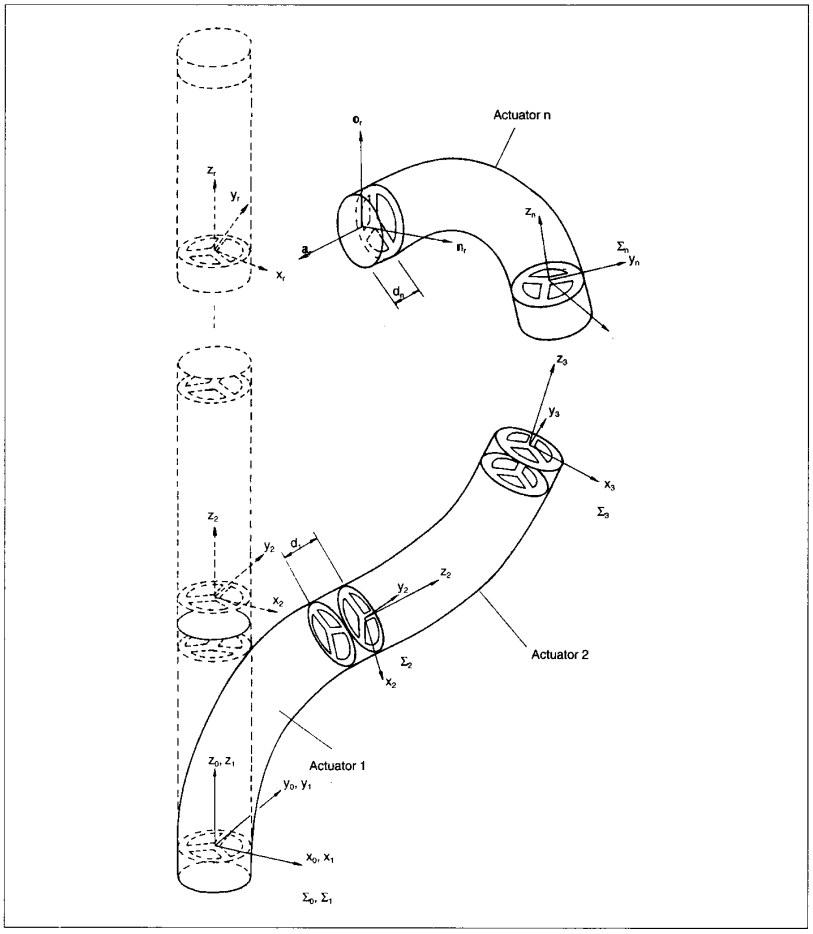

Fig. 8. Configuration of manipulator made of n FMAs.

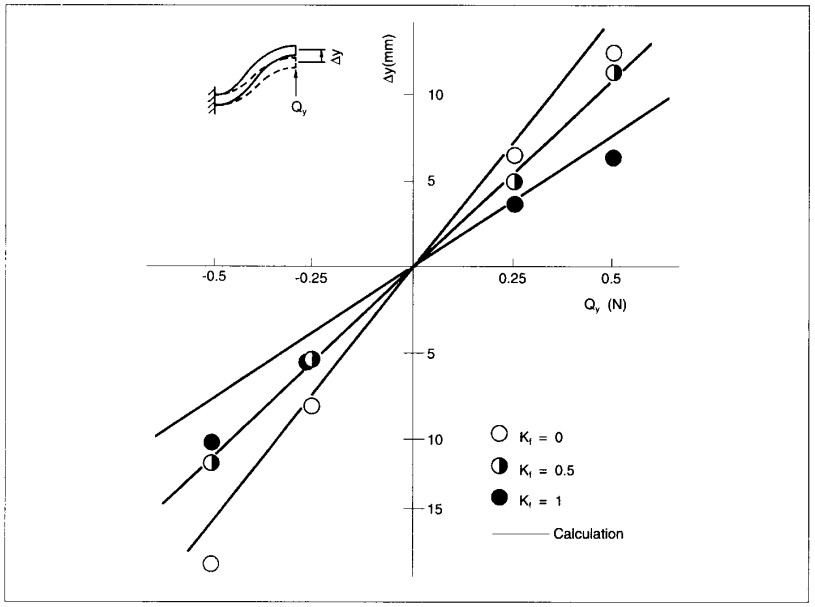

Fig. 9. Experimental result of feedback control.

Σ_i. K_1 and K_2 are specific parameters, depending on the FMA size and stiffness of the rubber, and are assumed constant for simplicity. From (8) we obtain the following equation:

$$\begin{pmatrix} P_{i1} \\ P_{i2} \\ P_{i3} \end{pmatrix} = \begin{bmatrix} 0 & (2/3)K_1 & (1/3)K_2 \\ 1/(\sqrt{3}K_1) & (-1/3)K_1 & (1/3)K_2 \\ -1/(\sqrt{3}K_1) & (-1/3)K_1 & (1/3)K_2 \end{bmatrix} \begin{pmatrix} {}^{i}x_i \\ {}^{i}y_i \\ {}^{i}z_i \end{pmatrix} \tag{9}$$

Transfer matrixes from the global coordinates Σ_o to the local coordinates Σ_i are expressed as follows, where α_i is the angle between the x_i-axis and x_o-axis; $\alpha_1 = (-3/4)\pi$, $\alpha_2 = (1/4)\pi$, $\alpha_3 = (-1/4)\pi$, $\alpha_4 = (-3/4)\pi$ [rad]:

$$\begin{pmatrix} {}^{i}x_i \\ {}^{i}y_i \\ {}^{i}z_i \end{pmatrix} = \begin{bmatrix} \cos\alpha_i & \sin\alpha_i & 0 \\ -\sin\alpha_i & \cos\alpha_i & 0 \\ 0 & 0 & 1 \end{bmatrix} \begin{pmatrix} {}^{o}x_i \\ {}^{o}y_i \\ {}^{o}z_i \end{pmatrix} \tag{10}$$

It is easy to control the hand using (9) and (10). First, the desired movements for the four FMAs are described in global coordinates Σ_o. Then, they are transferred to local coordinates Σ_i using (10). The internal pressure, required in each chamber, is calculated by (9).

Analysis of Stable Region for Holding

First, consider the weight holding capacity for the hand in the z_o direction. As shown in Fig. 12, the ith FMA is loaded with $Q_{\xi i}$ and Q_{zi} by the object. μ is the coefficient of static friction and g is the normal distance between the FMA and the object. Subscripts associated with ξi and zi mean a force in the ξ_i and z_i directions. $K_{\xi i}$ and K_{zi} represent the FMA tip compliances in the ξ_i direction for $Q_{\xi i}$ *and* Q_{zi}, respectively. $\xi_{oi}(P_{i1}, P_{i2}, P_{i3})$ is a function of P_{ij}, representing the tip position that the FMA would take without load.

For the ith FMA tip deflection caused by $Q_{\xi i}$ and Q_{zi}, the following equation is obtained:

$$K_{\xi i} Q_{\xi i} + k_{zi} Q_{zi} = g - \xi_{oi}(P_{i1}, P_{i2}, P_{i3}) . \tag{11}$$

A non-slip holding is defined as follows:

$$| Q_{zi}/Q_{\xi i} | < \mu \tag{12}$$

From (11) and (12), the following equation for weight capacity per FMA is derived:

$$\frac{g - \xi_{oi}}{K_{\xi i}/\mu + K_{zi}} < Q_{zi} < \frac{g - \xi_{oi}}{-K_{\xi i}/\mu + K_{zi}} \tag{13}$$

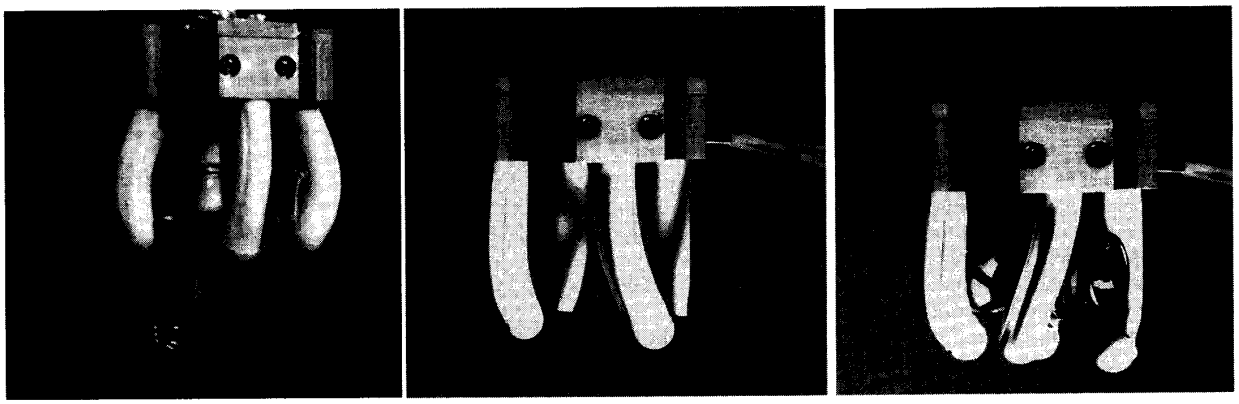

(a) (b) (c)

Fig. 10. Examples of holding mode. (a) Pinch. (b) Pair-pinch. (c) Grasp.

Next, consider stability in the pinching mode. When the working fluid pressure reaches some limit, an unstable phenomenon occurs; the object and FMAs turn unstable around the z_o-axis. This problem was analyzed under the simplification that the four FMAs move in the same way. (Then, subscript i is omitted in the following.)

Fig. 13 shows an equivalent model with eight springs, representing the pinching mode, where there are four contact points between the FMAs and the object. Each spring simulates the compliance for an FMA in the ξ,η–direction. The spring constants in the ξ,η direction are assumed to be equal here. This assumption is reasonable, because the FMA movements in the pinching mode are not so large.

Gripping force $Q\xi$, which an FMA exerts on an object, is simulated by adding compressionδ_o to the spring in the ξ-direction. Without $Q\xi$, the FMA tip would be located at $\xi o + K_z Q_z$ in the x-direction, when actually it is located at g. Then, the following is obtained:

$$\delta_o = \xi_o + K_z Q_z - g. \qquad (14)$$

The stability of an analytical spring model like this was analyzed in [7]. d_o is the FMA diameter and D is a diagonal distance between FMAs. Applying the result, the following stability condition is obtained:

$$\xi_o + K_z Q_z < (D - d_o)/2. \qquad (15)$$

It was found that the pair-pinch mode, shown in Fig. 10, is always stable.

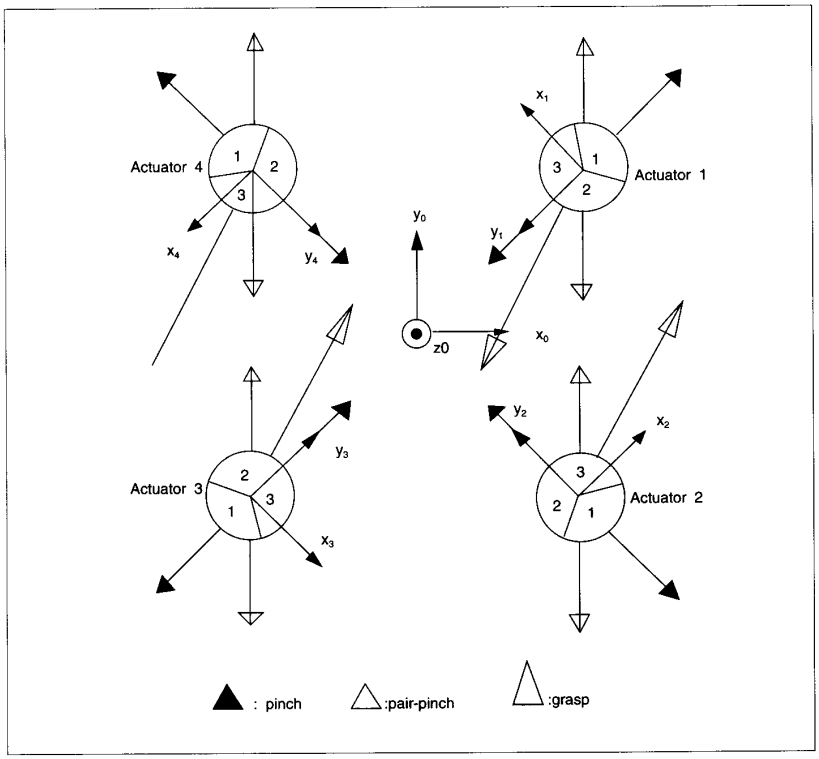

Fig. 11. Movement of fingers in holding mode.

Experiments

The theoretical results already described were compared with an experiment involving pinching a bronze cylinder 31.5 mm in diameter. The critical force Q_z for stability and the weight handling capacity were measured for each pressure P_1.

The results are presented in Fig. 14, where the critical slip point is marked with ○ and the critical stability point is shown by △. The theoretical results, shown in Fig. 14, were calculated with 1.5 as the coefficient of static friction. They agreed with an error of about 15%.

By using (9) and (10), not only can an object be held, as shown in Fig. 10, but also the object may be manipulated with the fingers. Fig. 15 shows a bolt being tightened. In experiments, the bolt turning speed was about 0.25 rps and the maximum torque was about 0.01 Nm. It is easy to

screw in a bolt by roughly setting the position and direction of the hand because of the high FMA compliance.

Distinctive Features

A new flexible microactuator (FMA) was applied to miniature robot mechanisms. Small gentle robot mechanisms without conventional links can be designed by using these FMAs.

An FMA and robot mechanisms made from FMAs have several distinctive features, when compared with conventional robot mechanisms. 1) They are easy to miniature because of their simple structures. 2) They have a high power density. 3) They have many degrees of freedom; pitch, yaw, and stretch, suitable for robot mechanisms. 4) They are cheap. (They can be used as disposable robots for medical use.) 5) They operate smoothly and gently, because of their frictionless mechanisms. 6) It is easy to construct miniature robots, because FMAs also act as robot structures.

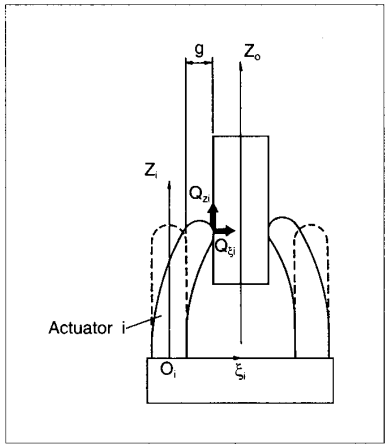

Fig. 12. Analytical model of holding.

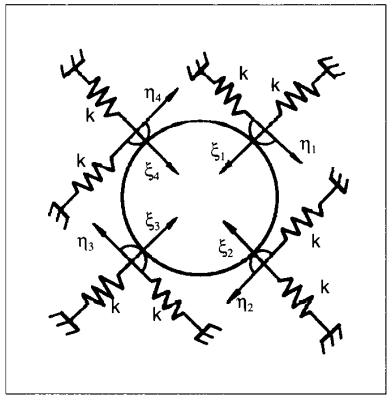

Fig. 13. Equivalent model of pinching mode.

FMAs are expected to be applicable for use in miniature robotic mechanisms, where space is restricted or gentle handling is required.

Acknowledgment

The authors would like to thank Y. Nogiwa for his encouragement, and also S. Sekiguchi for his assistance in device fabrication.

References

[1] I.W. Hunter *et al.*, "Manipulation and dynamic mechanical testing of microscopic objects using a tele-micro-robotic system," *IEEE Control Syst. Mag.*, vol. 10, pp. 3-9, Feb. 1990.

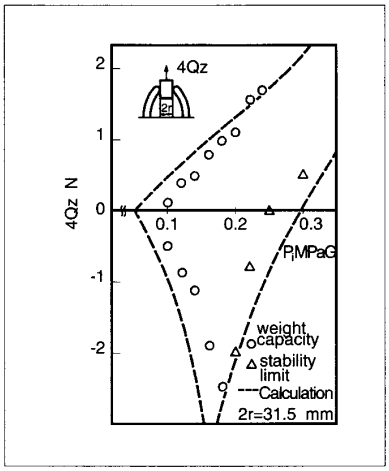

Fig. 14. Weight holding capacity and stable region for pinching.

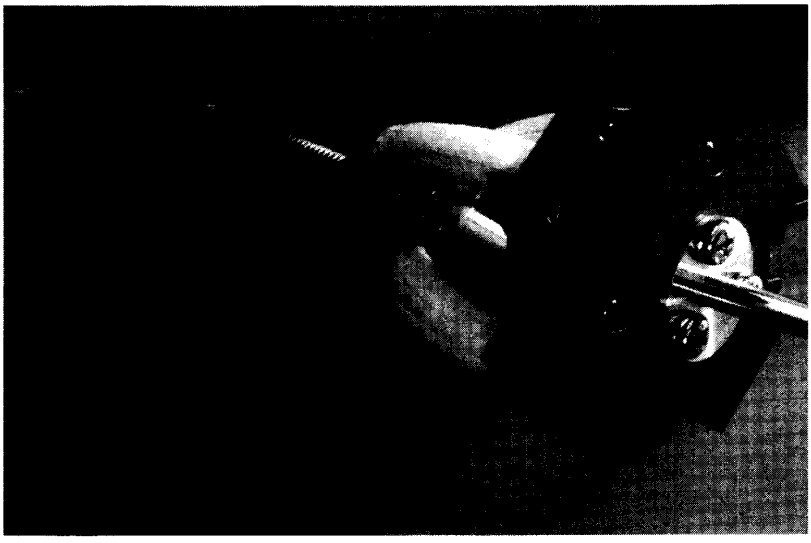

Fig. 15. Bolt-screwing experiment.

[2] K. Suzumori *et al.*, "Flexible microactuator for miniature robots," in *Proc. 1991 IEEE Worksp. Micro-Electro Mechanical Syst.*, pp. 204-209, Jan. 1991.

[3] K. Suzumori, "Flexible microactuator (1st Rep., Static Characteristics)," *Trans. Japan Soc. Mech. Eng.*, vol. 55, no. 518, c, pp. 2547-2552, July 1989 (in Japanese).

[4] K. Suzumori, "Flexible microactuator (2nd Rep., Dynamic Characteristics), *Trans. Japan Soc. Mech. Eng.*, vol. 56, no. 525, c, pp. 1887-1893, Oct. 1990 (in Japanese).

[5] H. F. Shulte, Jr., "The characteristics of the Mckibben artificial muscle," *The Application of External Power in Prosthetics and Orthetics*. 1960, pp. 94-115.

[6] T. Fukuda *et al.*, "Rubber gas actuator driven by hydrogen storage alloy for In-pipe inspection mobile robot with flexible structure," in *Proc. IEEE Int. Conf. Robotics and Automation*, pp. 1847-1852, 1989.

[7] M. Kaneko *et al.*, "A realization of stable grasp based on virtual stiffness model by robot fingers," in *Proc. IEEE Int. Worksp. Advanced Motion Control*, 1990.

Koichi Suzumori was born in Kanazawa, Japan, in 1959. He received the M.S. degree in 1984 and the Ph.D. degree in 1990 in mechanical engineering from Yokohama National University. Since 1984, he has been employed by Toshiba Corporation. Currently he is a Research Scientist at the Mechanical Engineering Laboratory, Research and Development Center. His research interests include

teleoperation, microrobotics, new actuators, and pneumaticdevices.

Shoichi Iikura was born in Nagasaki, Japan, in 1948. He received the B.S. degree in mechanical engineering from Tokyo Institute of Technology in 1971. He has been employed at Toshiba Corporation since 1971 and has been a member of the Mechanical Engineering Laboratory, Research and Development Center. Since 1982, he has been a member of the Mechatronics Section at the Mechanical Engineering Laboratory, RDC, and has been in charge of development of the remote manipulator systems for hazardous environments such as nuclear and space. His research interests are in the area of drive mechanisms of mechanical systems including actuators. Currently he is the Senior Research Scientist of the Mechatronics Section at the Mechanical Engineering Laboratory.

Hirohisa Tanaka is a Professor in the Machine Design Division of Yokohama National University in Japan. He received the M.S. degree in 1972 and the Ph.D. degree in 1975 in mechanical engineering from the University of Tokyo. He was also a Lecturer in the Fluid Power Control Division of the Institute of Industrial Science of the University of Tokyo from 1975-1979. He has developed electrohydraulic components for automotive and medical applications, and recently successfully developed a traction drive continuously variable power transmission for a passenger car with 200 kW engine power.

Out of Control

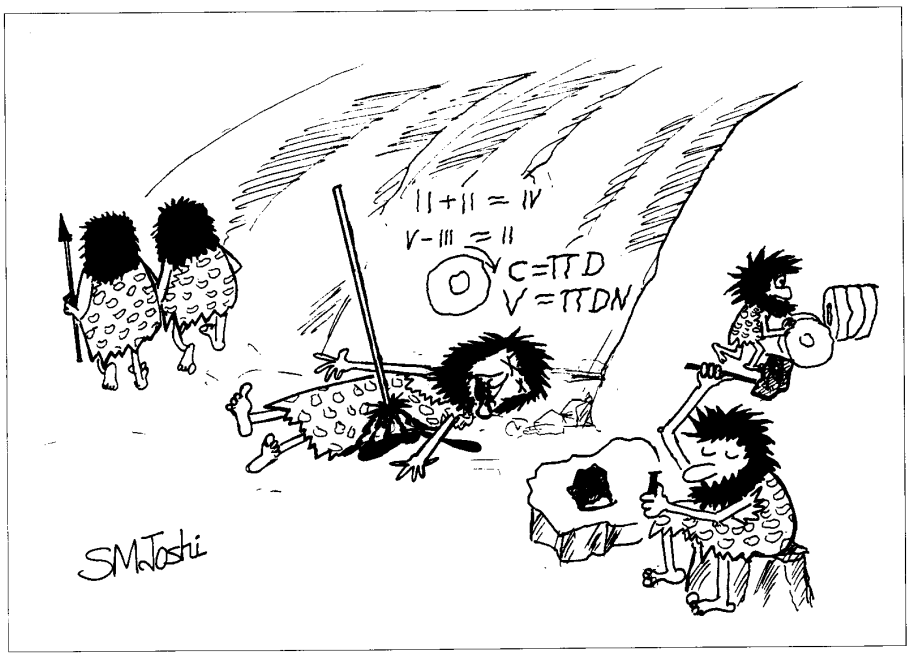

Phrragg receives disciplinary action for engaging in esoteric research.